We are IntechOpen,
the world's leading publisher of
Open Access books
Built by scientists, for scientists

6,900
Open access books available

186,000
International authors and editors

200M
Downloads

Our authors are among the

154
Countries delivered to

TOP 1%
most cited scientists

12.2%
Contributors from top 500 universities

CLARIVATE ANALYTICS
BOOK CITATION INDEX
INDEXED

WEB OF SCIENCE™

Selection of our books indexed in the Book Citation Index
in Web of Science™ Core Collection (BKCI)

Interested in publishing with us?
Contact book.department@intechopen.com

Numbers displayed above are based on latest data collected.
For more information visit www.intechopen.com

Synthesis of NPs by Microemulsion Method

Antonio Cid

Abstract

Microemulsions are self-aggregated colloidal systems that provide a controllable system with a promising application as nanoreactors: they can act as pools within which the properties of the nanoparticles can be controlled without difficulty. So in this chapter, I will deal with the metal NPs synthesized by the microemulsion method. This method allows in some cases to control the properties of size, shape, and crystal structure of the metallic NPs, thus generating with the same reagents a series of seeds of different shapes and sizes. The control of the reaction time, the temperature, and the reaction conditions will give us a production of different geometries that will find different applications in large range of research fields.

Keywords: microemulsion method, nanoparticles, colloidal suspensions, self-assembly, surfactant

1. Introduction

During the last decades, self-assembly of micro- and nano-materials attracted a widespread mindfulness because of special properties when comparing with bulk counterparts, because of mechanical and physicochemical property changes at micro- and nanoscale. I will focus on a particular three-phase diagram proportion that is known as the microemulsion system. It is thermodynamically stable and isotropic dispersion of two immiscible liquids, where a surfactant stabilizes micro-domains [1]. It includes different structures and configurations corresponding to different performances of self-assembled colloidal systems. Then I will focus on the assembled structure of nanoparticles. To be able to obtain these structures by microemulsion method, it must be known making a good use of the properties of the microemulsion systems, in which the composition of these structures will determine properties as important as the size of the microdroplets. That ultimately will determine the reaction system of our synthesis of nanoparticles.

The microdroplet environment offers a controllable medium to obtain NPs with tailored size, shape, and structural properties.

2. Metal nanoparticles (MNPs)

2.1 Anionic surfactants

Here I focus on MNPs synthesized by microemulsion method using the anionic surfactant, reviewing literature that employed this surfactant type I found a very noticeable research.
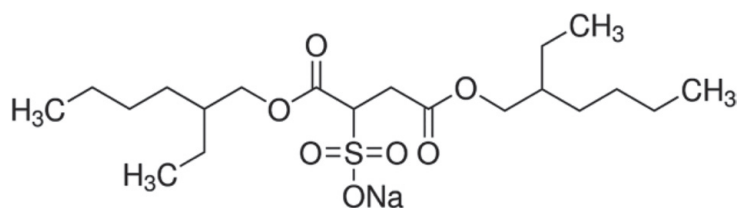
Figure 1.
AOT chemical structure.

Microemulsion method was used by Kon-No et al. [2]; they prepared two microemulsions, one them solubilizing $FeCl_3$ aqueous solution in AOT/cyclohexane and the other aqueous NH_3 in AOT/cyclohexane; both were mixed joint (see AOT chemical structure in **Figure 1**). To obtain the formation of Fe_3O_4 in the micelle, authors added a $FeCl_2$ solution to the mixture of two microemulsions. The solution showed stability during 2 years. A diluted solution of the colloid obtained was characterized by TEM to determine the crystal structure and size distribution by electron micrography. Then the authors obtained magnetic measurements together with an extended analysis to determine detailed surface magnetic properties that allowed them to conclude that (i) distribution function of colloidal particles is a log-normal type, coincidentally with results obtained by gas evaporation technique, (ii) the magnetic interaction between the colloidal particles is negligible, (iii) the colloidal system showed superparamagnetism about 50K, (iv) paramagnetic Fe ions potentially are present on a particle surface, and (v) the temperature dependence of the spontaneous magnetization linearly decreases with the increase of temperature.

López-Quintela and Rivas [3] reported a simple and powerful method to obtain ultrafine particles by means of chemical reactions in microemulsions. The reaction happened within the nanodroplets of the microemulsion. Varying droplets' radii authors were able to control particle dimension. They reported that the proper selection of microemulsion components would ease the exchange of reagents between the "transition dimers" formed by two droplets of the microemulsions; for this to happen, an important alteration in the local curvature is necessary, so the selection of adequate surfactants that shows a radius of curvature close to their natural radius will facilitate the opening of channels [4–9], particle formation, and growth. Once the particles are formed, the surfactant particles act as surface agents, limiting the future growth of the particles. The sizes of the microemulsion droplets can be tuned between 5 and 50 nm by changing the relation of the components of the microemulsion (e.g., $W = [H_2O]/[AOT]$) or varying the microemulsion itself. The results for Fe particles obtained in an AOT microemulsion system ($W = 22.2$; $[AOT] = 0.05$ M; reactant A: $[FeCl_2] = 1.9 \times 10^{-4}$ M; reactant B: $[NaBH_4] = 8.8 \times 10^{-4}$ M) were discriminated using XRD. Nucleation process was confirmed by enhancing the number of scattering centers and hence the scattering intensity. Conversely, growth of the particles is associated with a decrease on the scattering intensity because of the "disappearing" of the smaller particles during their growth. The authors concluded that this general method produces ultrafine particles with tunable size by means of chemical reactions within microemulsions. This simple and reproducible method allowed them to produce quasi-monodisperse particles, within a thermodynamically stable system (microemulsion) that was used to control the growth of the particles.

Mann et al. reported [10] that interfacial activity could be used to combine nanoparticle synthesis and self-assembly to produce complex organized materials rising from the interaction of tensioactive molecules attached to specific nanoparticle crystal faces. Authors demonstrated this principle by controlling the $[Ba^{2+}]:[CrO_4^{2-}]$ inside of droplets of the microemulsion that tunes the fusing
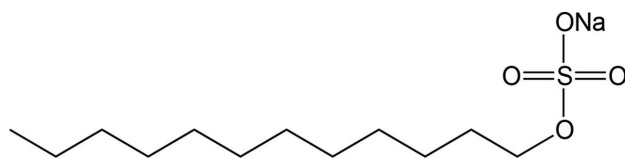
Figure 2.
SDS chemical structure.

of microdroplets and reverse micelles. It allowed them to produce linear chains, rectangular superlattices, and long filaments, as a function of reactant ratio. They carried out the synthesis and self-assembly of NPs by converting sodium AOT to Ba(AOT)$_2$ by direct precipitation [11].

Wang et al. [12] reported by the first time a new microemulsion method to synthesize magnetite NPs. The novelty of their method founded on the cost-effective use of a single microemulsion. The authors prepared the microemulsion by solubilizing NaOH solution into DBS/ethanol/toluene system (DBS, sodium dodecylbenzene sulfonate), and then ferric and ferrous salts with molar ratio (2:1) were made into a mixed solution. A volume of this mixture was drop-wise added to microemulsion under vigorous stirring. The mixed system turned black immediately. After the mixed system was stirred during ½ h and then left undisturbed during 5 h, a two-layer system appeared. The upper layer was black, which contained the NPs, and lower layer was discarded. Following a magnetic separation technique, the magnetite NPs were extracted and then washed several times in ethanol/water solution (1:1) to obtain magnetite NPs.

He et al. reported [13] the chemical synthesis of a nonviral gene transferor, calcium carbonate NP using SDS microemulsions (see SDS chemical structure in **Figure 2**) [14, 15].

2.2 Cationic surfactants

Here I focus on MNPs synthesized by microemulsion method using the cationic surfactant, examining literature that employed this surfactant type I found very outstanding research.

Chin and Yaacob [16] reported the synthesis of magnetic iron oxide nanoparticles by preparing water-in-oil microemulsion system. Authors investigated two different volumetric ratios of Fe^{2+} and OH^- (1:1 and 2:1). Crystallized, physical, and magnetic sizes of magnetic iron oxide nanoparticles were in the superparamagnetic size range (XRD, TEM, and AGM). Superparamagnetic behavior was warranted by hysteresis loop nonappearance in magnetization curve at room temperature. MIONPs were obtained by Massart's method too. The saturation magnetization of MIONPs obtained by *w/o* microemulsion system was larger though the crystallization size was lower, which demonstrated that MIONPs could be custom-made by distinct methods.

The preparation of iron oxide NPs was carried out according to the following route. Ferrous chloride salt solution was prepared (0.2 M); it was steady by adding a few drops of hydrochloric acid (0.5 M). Afterward, the microemulsion was set by melting HTAB in n-octane; subsequently 1-butanol was added followed by FeCl$_2$ aqueous salt solution. The system was gradually shaken till a clear microemulsion suspension was attained. By repeating above method a microemulsion containing 0.25 M NaOH solution was produced.

These microemulsion systems were next fused at 1:1 vol. Instantaneously, a dark green solid was produced before it turned to black. The NPs were gathered and later cleaned repeatedly with acetone and de-ionized water and then they were dried at room temperature which is called S1. The same route was followed to yield a second sample with primary [Fe^{2+}] = 0.1 M. [NaOH] was kept at 0.25 M. The volumetric

proportion of microemulsion containing Fe^{2+} to microemulsion containing OH^- was 2:1. The sample was called S2 [17]. To compare, by Massart's procedure, S3 has been obtained [18]. Magnetic iron oxide NPs (MIONPs) were effectively formed at r.t. with microemulsion method. The MIONPs showed spherical shape. From the results of TEM, AGM, and XRD, the crystallite, physical, and magnetic sizes of the MIONPs were <10 nm. The mean physical size for S1, S2, and S3 is 6.5, 4.2, and 8.7 nm, respectively. The rise of the total number of microemulsion produced smaller particles. Particles produced by microemulsion procedure were smaller in size and showed higher saturation magnetization, compared to the particles obtained by Massart's procedure.

Shen et al. [19] prepare CTAB-stabilized gold nanowires and nanoparticles with a networked structure and different shapes using in situ *n*-butanol reduction in $CTAB/n$-butanol/n-heptane/$HAuCl_4$(aq) through microwave dielectric heating (XRD, UV-vis, and TEM). The shape of the hydrophobic gold nanocrystals was effectively modulated tuning of $CTAB/HAuCl_4$ ratios. Anisotropic gold nanostructure formation mechanism was deliberated, which confirmed that CTAB (**Figure 3**) perform a preeminent key role in the drummed-up gold nanowires.

With the decrease of W, the shapes of gold nanocrystals obtained by this method changed from sphere-like decahedron nanoparticles to nanowires with a networked structure. It was revealed that $AuCl_4^-$ cation and ion of surfactant CTAB played key roles on formation and stabilization of the shape of gold nanowires. The attracting force among gold nanoparticles, which also caused an orienting growth of gold nucleus, was caused by the preferential adsorption of $AuCl_4^-$ and the selective adsorption of CTAB on the facets of preliminary gold particle surface. This method novel and simple for synthesizing gold nanowires with a networked structure is expected to be appropriate to the synthesis of other metals to attain novel nanostructures.

Sharma et al. [20] reported a detailed and complete study on the growth kinetics of iron oxalate nanorods as they formed throughout several days inside the water pool of CTAB microdroplets (MDs) in isooctane. Authors underlined the novelty of this experimental study on nanostructure preparation in microemulsion-based reactions that could explain the key role of droplet interplay in the reaction kinetics. DLS, TEM, and FCS characterization was completed throughout some days to follow the whole growth kinetics of iron oxalate nanorods beginning from their particle nucleation. Considering the FCS data with an appropriate kinetic model, the droplet-fusion time or dimer lifetime 28 µs was obtained along with the droplet melting rate and the equilibrium constant of the chemical reaction. The droplet association rate exhibited a noteworthy time dependency that straight relates it to the growth mechanism. Combining FCS, DLS, and TEM, three different periods in the complete nanorod growth kinetics appeared: (i) a prolonged nucleation-dominant NP growth period, then (ii) a short period where isotropic NPs shifted to anisotropic growth to form nanorods, and (iii) finally the period where droplet-fusion-assisted elongation of nanorods was proved. The detailed methodologies discussed in this study could be applied to understand the growth kinetics of nanostructures, which are required for various applications in nanoscience and nanotechnology.
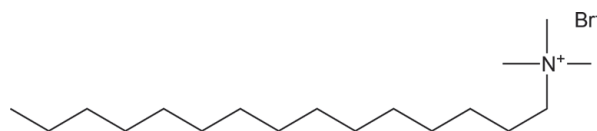

Figure 3.
CTAB chemical structure.

2.3 Nonionic surfactants

Here I review the literature about the use of nonionic surfactants as stabilizer/emulsifier of the microemulsion involved on the synthesis of MNPs by microemulsion method.

Sanchez-Dominguez et al. [21] reported a novel and direct approach to synthesize inorganic NPs at ambient conditions using *o/w* microemulsions to dissolve organometallic precursors. Addition of reducing or oxidizing/precipitating agents implies the formation of metallic or metal oxide nanoparticles, respectively. The authors chose nonionic aggregates and several strategic compositions for nanoparticle synthesis at 25°C. HREM shown that small metal NPs (Pd, Pt, and Rh) and nanocrystalline metal oxide NPs (Ce(IV) oxide with cubic crystalline structure confirmed by XRD) of <7 nm can be obtained at atmospheric pressure and 25°C.

Capek reviewed water-in-oil microemulsion method to prepare metal NPs [22]. This technique allows preparation of ultrafine metal particles ranging in the size diameter between 5 and 50 nm. Author reviewed the previous literature on particle synthesis of various metals such as silver, copper, cadmium, cobalt, nickel, cadmium, and gold in the reverse microemulsion systems. The precursor metal salts and reducing agents are mainly water-soluble molecules, and consequently the MNP nuclei formation progresses in the water microdroplets. The rate of the nuclei formation of the particle depends on the percolation degree of microemulsion droplets. Effects of stabilizer nature and concentration, the oil phase nature, reducing agent, and additive on the NP synthesis are shortened and assessed. The impact of numerous factors such as temperature, the metal salt nature, the incident light, and reaction conditions were also revised.

Tan et al. [23] reported the microemulsion application to prepare silica-coated iron oxide NPs using nonionic surfactants (Triton X-100, Igepal CO-520, and Brij-97, their chemical structure can be observed in **Figures 4–6**, respectively) for the preparation of microemulsions. Iron oxide NPs are formed by co-precipitation.
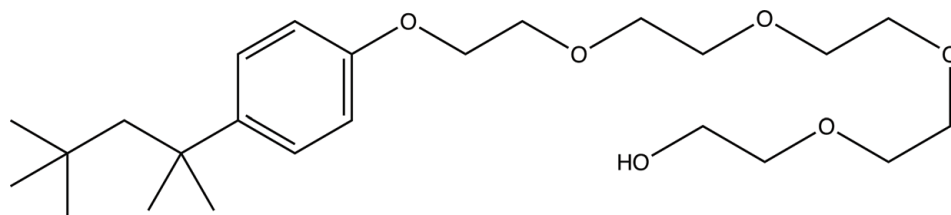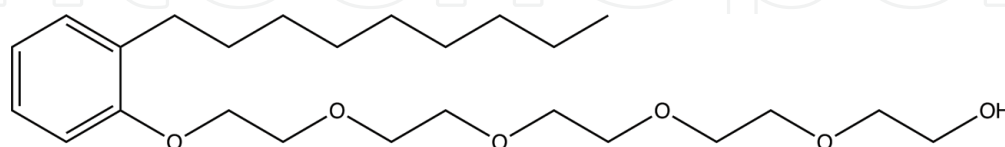
Figure 4.
Triton X-100 chemical structure.

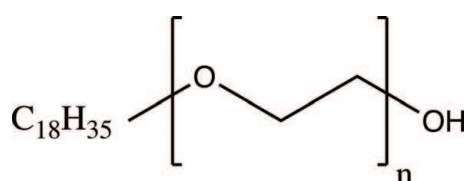**Figure 5.**
IGEPAL CO-520 chemical structure.

Figure 6.
Brij 97 chemical structure.

Figure 7.
1-Tetradecane chemical structure.

TEM, XRD, and SQUID magnetometry were used to assess both uncoated and silica-coated FeO NPs. Particles displayed magnetic properties near to that of super-paramagnetic materials. By using this route, magnetic NPs ranging 1–2 nm and with very monodispersed in size (percentage std. <10%) were obtained. Base-catalyzed hydrolysis and the polymerization reaction of tetraethyl orthosilicate (TEOS) in microemulsion were used to produce a uniform silica coating of 1 nm enclosing the naked NPs.

Khiev et al. [24] reported the synthesis of regular shape and monodispersed nickel sulfide (NiS) NPs were made in *w/o* microemulsion system including sucrose ester (S-1170) as the nonionic surfactants (which is a nontoxic and biodegradable). NiS NPs were characterized by EFTEM, XPS, and UV-Vis-NIR. NPs showed size ranged between 3 and 12 nm.

The typical microemulsion used in their synthesis had a composition of 28, 56, and 16 wt% of tetradecane/1-butanol (see chemical structure in **Figure 7**) and of aqueous solution containing $Ni(NO_3)_2$ and Na_2S, respectively. The hastened fine particles achieved from centrifugation were cleaned with absolute ethanol and distilled water leastwise fivefold so as to wash away the excess tensioactive byproducts and unreacted reagents. The products were dried in vacuum oven for 16 h at 50°C till a constant weight was attained. It was denoted that the size of the NPs enhanced with the reactants' concentration due to the fusion of nuclei. The presence of quantum confinement effect was apparent for the resultant NPs as the likely bandgap energy exhibited noteworthy increase. Sugar-ester-based nonionic microemulsion offers proper micro-medium to formulate NPs with narrow size distribution and high uniformity.

Pine-Reyes and Olvera reported [25] the use of human and environmentally friendly *w/o* microemulsions to synthesize ZnO NPs based on a not complex procedure (Span 80 and Tween 80 mixture—**Figures 8** and **9**). The method lets achieving NPs with a mean size of approximately 31.2 nm, with low range size variation and pseudo-spherical morphology. XRD, SEM, and TEM confirmed ZnO hexagonal wurtzite phase. The microemulsion organic phase was formed by the mixture of different proportions of emu oil and surfactant (1:1, Span 80, Tween 80) (see their chemical structures in **Figures 8** and **9**, respectively). Next, an aqueous solution of ZnAc (0.5 M) was slowly drop wised to the previous mixture. The systems were mixed under magnetic stirring (1200 rpm, 5 min) and later stored 24 h at r.t. The ZnO powders were synthesized by the drop-wised addition of a (aq) solution of NaOH (1.0 M) to previous prepared microemulsion. NaOH acted as precipitating agent. The mixture was maintained at 60°C and stirred at 1200 rpm for 5 min. In this step, NaOH diffused into the continuous phase achieves the oil-solution interface, which eased the formation of ZnO. Then, mixtures were successively washed by centrifugation at 7500 rpm in water, hexane, and acetone to separate oil and surfactant residues and byproducts from precipitates. Finally, the precipitates were dried during 1 h at 100°C and then calcined by 2 h at 800°C.

Sample M10 with 15% ZnAc, 55% surfactant, and 30% oil exhibits the smallest average particle size, 31.2 nm, and a distribution of 41.2 nm. SEM and TEM micrographs have demonstrated a pseudo-spherical morphology. XRD analysis confirms that samples presented a hexagonal wurtzite phase with preferential growth
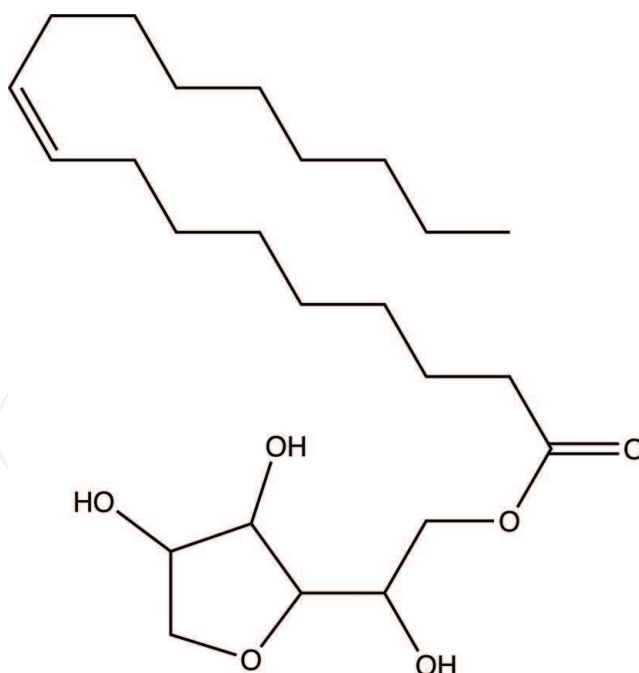
Figure 8.
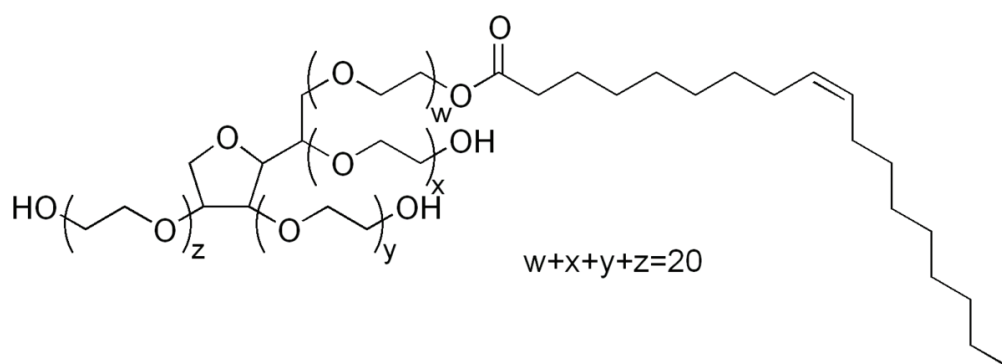*Span 80 chemical structure.*

$$w+x+y+z=20$$

Figure 9.
Tween 80 chemical structure.

direction [101]. The results showed that this method is a suitable pathway for ZnO NPs synthesis. Moreover, it is a simple, direct, and cost-effective method for obtaining nanostructured materials with small particle size and narrow size distribution particle.

3. Silica nanoparticles

Here we focus on a metalloid and the use of microemulsion method to obtain silica NPs. Yamauchi et al. [26] reported the synthesis of ultramicroparticles of silica by means of *w/o* microemulsion method.

Shantz et al. reported [27] synthesis of silicalite-1 nanocrystals in AOT-based microemulsion. They demonstrated that anionic microemulsions drive to essentially distinct crystal patterns than the nonionic [28] or cationic microemulsions formerly explored. The authors concluded that AOT and SDS anions synthesized by microemulsion method were employed to crystallize silicalite-1 nanocrystals with well-defined shapes and structures. Box, disk-like, spherical, and twinned nanocrystals were found under distinct experiential circumstances. It was also shown that tensioactive

uniqueness, TPAOH content, and the presence of salts and co-surfactant influence the morphology and crystallinity of silicalite-1. The crystal size and shape contrasted in all cases than those prepared in default of the microemulsion. The crystal morphology could be regulated by adjusting the interplay among surfactant and zeolite surfaces.

4. Outlooks and perspectives

Here I focus on the state-of-the-art research on nanotechnology that involves the microemulsion method.

Chen et al. [29] reported the synthesis of CdS QDs by means of a chemical reaction between amide of cadmium acetate dehydrate and thioacetamide by using a microemulsion-based hydrothermal method. Their properties could be tailored through the use of Emulsifier OP and CTAB, which yield a usual cubic phase and a scarce hexagonal phase, apiece. Authors explored a possible mechanism involving the critical role of surfactant in the formation of crystal structure. A direct dependence of the crystal size that regularly increased with the increase of temperature is also found, and the appearance of red shift in the absorption and emission peaks confirmed the quantum confinement effect. All the desired properties of CdS QDs synthesized by this route denote the chance of the preparation of high-quality QDs under the appropriate reaction conditions.

First, aqueous solutions 0.005 M of cadmium acetate and thioacetamide were set by melting in deionized water with the aid of magnetic stirrer. Next, two reverse microemulsions (M_{Cd} and M_S) with different aqueous phases were prepared. Either M_{Cd} or M_S enclosed three mutual constituents in the volume ratio of 3:5:20, that is, a surfactant of CTAB or emulsifier OP, co-surfactant of n-butyl alcohol, and a continuous oil phase of n-hexane. Once jointly mixed under constant stirring at r.t. during 30 min, it was moved into a 100 mL Teflon-lined autoclave with hydrothermal treatment at 70–120°C for 13 h, succeeded by chilling at r.t. readily. The yellow precipitants were harvested from the synthesis medium by centrifugation, cleaned with anhydrous ethanol and deionized water sometimes and then dried at 70°C, to finally obtain CdS QDs.

The crystal structure was characterized by XRD, obtaining OP at 2θ values of 26.5, 43.9, and 52.1° which agree with the (1 1 1), (2 2 0), and (3 1 1) planes of cubic structure. The morphology was analyzed with a transmission electron microscope, denoting that at 70°C, the mean crystal size of CdS QDs is much tinier ($\approx$3 nm), and afterward it achieved 5.9 nm, when the temperature was increased to 120°C. It noticeably proved the influence of reaction temperature on the crystal size of the as-prepared CdS QDs. The optical properties of samples were characterized by the UV-4100 spectrophotometer and FLS920 steady-state and transient fluorescence spectrometer. In addition, infrared spectroscopy was recorded.

Wei et al. [30] reported the synthesis of the core-shell $NaGdF_4$@$CaCO_3$-PEG NPs were carried out through a facile microemulsion method with using $NaGdF_4$ NPs as templates [31]. Concisely, 5 mL $NaGdF_4$ NPs, 10 mL of cyclohexane, 3.45 mL of Triton X-100, and 3.2 mL of 1-hexanol were added to a flask and combined carefully, followed by annexing 800 μL of a 30 mM solution of $CaCl_2$ to obtain a well-dispersed *w/o* microemulsion. Before the 40 μL, 2.92 M solution of sodium carbonate was added. The microemulsion was kept under mild stirring for 8 h of the mix; the $NaGdF_4$@$CaCO_3$ NPs were gathered by centrifugation and next re-dispersed in 10 mL of ultrapure water. Afterward, 2 mL and 0.2 M PEG8000 (aq.) solution was annexed and stirred for additional 8 h, and subsequently the NPs were gathered by using centrifuge at 10,000 r.p.m. during 15 min and re-dispersed in 20 mL of ultrapure water for further purpose.

In this work, a core-shell nanoparticle of $NaGdF_4@CaCO_3$-PEG was designed as an activable MR/US dual-modal imaging contrast for cancer diagnosis, which is activated by the acidic environment. Authors used the coating of $NaGdF_4$ with a layer of hydrophobic $CaCO_3$ to limit water availability, thus quenching the sphere Gd^{3+} relaxation effects, with the aim of achieving this OFF/ON responsive MR imaging behavior. At acidic aqueous solution, $CaCO_3$ was melted to produce CO_2 bubbles, which is applied to obtain US signal. While a robust MRI augmentation could be triggered on dissolution of $CaCO_3$ and discharge of the earlier quieted $NaGdF_4$ in the aqueous solution. In vivo results confirmed the heavy dual-modal magnetic resonance/ultrasonic imaging capabilities of $NaGdF_4@CaCO_3$-PEG at the tumor area with an acidic environment. Authors expected that their findings might deliver a novel sight for approaches to developing NPs with reactive dual-modal imaging skills. The here-described proof-of-concept nanoparticles with pH-triggered magnetic resonance/ultrasonic dual-modal imaging improvement may assist as a useful guide to advance various molecular imaging strategies for cancer diagnosis in the future.

Majumder and Roy reported the synthesis of mesoporous CeO_2 nanospheres [32] with noticeably raised surface area. It was ready using reversed micelles by a water-in-oil microemulsion method. The structure and semiconducting properties of the NPs are accurately explored using TEM, FESEM, XRD, and UV-Vis. Despite after high-temperature burning, the structural holding of the nanomaterial was evident by EM. Comparing to those of other sensors of the same type, outstanding performances in terms of sensitivity, response-recovery times, and selectivity were found on the distribution of undoped CeO_2 nanospheres for the detection of low-ppm CO. These CO sensors showed 52% sensitivity with a reply time of only 13 s. The sensor parameters were analyzed as a function of both gas concentration and temperature. In addition to that on the scalable and cost-effective synthesis of CeO_2 nanospheres, authors also reported on the fabrication of packaged CO sensors, which could be potentially used for industrial and environmental monitoring purposes. To carry out the material synthesis, all of the chemicals (analytical grade) were applied without further treatment. Primarily, a microemulsion was formed by merging n-hexane, n-butyl alcohol, and diethyl ether in the weight ratio 3:2:1, energetically stirred till the mix turns out to be clear. The quantity of CTAB to reach critical micelle concentration (CMC) was calculated applying the standard conductometric method, where a sequence of microemulsions were examined changing the [CTAB] between 0.2 and 1.5 g. Then, 10 mL of 1 M aqueous solution of $Ce(NO_3)_3$ including 0.65 g of CTAB was annexed to the mix, and then it was agitated again till it showed transparency. Concurrently, another aqueous solution of 10% (w/v) NH_4OH was prepared. The above solutions were merged strongly till it forms a colloidal suspension. The material was gathered by centrifugation at 6000 r.p.m. during 30 min and consecutively washed using deionized water in an ultrasonic bath during 2 h. Lastly, the collected material was dried under vacuum and calcined at 600°C during 4 h.

Wang et al. reported the synthesis and applications of new biomimetic hybrid nanoplatform with theranostic agents [33]. Authors reported the synthesis of this nanoplatform; it was out by the next method: Silica NP core was used to encapsulate fullerene (C60) by a reverse microemulsion method. First, hexanol, Triton X-100, cyclohexane, and deionized water were jointly mixed. A total volume of 2 mL of fullerene in toluene (2 mg mL^{-1}) was then added into the mixture. Subsequently, 60 mL of ammonium hydroxide solution (28 wt%) and 100 mL TEOS were serially annexed, and the sample was rattled at 800 r.p.m. using a mini-stir bar during 24 h at r.t. Finally, the sample was annexed in 30 mL of ethanol to cease the reaction. The obtained sample was centrifuged at 13,800 × g during 10 min to attain fullerene-inserted silica C60S-NPs. After twofold cleaning with deionized water and ethanol, the NPs were suspended in 3 mL of ethanol and followed by the addition 20 mL of

APTMS. The mixture was stirred using a mini-stir bar (200 r.p.m., during 12 h) at room temperature to acquire the APTMS-coated C60S, C60S-A NPs. Lastly, the sample of C60S-A NPs was merged with DPPC liposomes and shacked for 5 h (r.t.) to harvest the phospholipid bilayer-coated C60S, LC60S-NPs. The LC60S NPs were gathered by centrifuging at 13,800 × g for 10 min. The DPPC liposomes were prepared by hydrating a thin DPPC film. Subsequently sonication for 2 min using a Branson 450 Sonifier, the sample of DPPC (1,2-dihexadecanoyl- sn-glycero-3-phosphocholine) liposomes (≈100 nm) was filtered throughout a 0.2 mm filter earlier mixing with the solution of C60S-A nanoparticles. I carried out a research on re-dispersion and self-assembly of C60 pointed special performance and arrangement depending on the solvent nature [34].

Authors concluded that both the encapsulation efficiency (EE) and minimal drug loading content (LC) of theranostic agents are vital calibers of multifunctional NPs for drug transfer. To attain great EE, low drug-to-NP provision ratios have frequently been applied for encapsulation, which outcomes in low drug LC. Authors designed a eukaryotic cell-like nanoplatform or EukaCell, which can be applied to attain great EE (≈100%) and LC (up to ≈87%) of theranostic agents (DOX and ICG). The release of the encapsulated drug can be exactly controlled using NIR laser irradiation to minimize the potential side effects. With the biomimetic eukaryotic cell-like configuration, the EukaCell had an extended half-life and strong stability in blood circulation and could favorably accumulate in tumor following intravenous injection. Finally, the drug-laden EukaCell displayed excellent safety and efficacy for cancer therapy. Authors demonstrated the tremendous potential of their EukaCell for providing theranostic agents to detect and treat cancer.

Tianimoghadam and Salabat reported the formulation of new microemulsion to prepare thiol-functionalized AuNPs [35]. The microemulsion system was obtained by mixing a yellow aqueous solution of 0.03 M of $HAuCl_4$ and a 0.05 M solution of TOAB/toluene. The same microemulsion containing 0.4 M of $NaBH_4$ was prepared independently and drop-wised under energetic stirring into the microemulsion enclosing metal ions. The formation of AuNPs was confirmed by the appearance of a stable light-ruby-red color resulting in microemulsion when the reduced Au(III) ions changed. To form a thiol monolayer surrounding the AuNPs, dodecanethiol (17 mg) was added while kept stirring during 1 h. To eliminate all residual TOAB surfactants (see TOAB chemical structure in **Figure 10**) and thiols from the AuNP surfaces, the AuNPs were pipetted into a 10 mL vial along with 3 mL ethanol and then centrifuged. This procedure was sixfold repeated, after which the dodecanethiol-stabilized AuNPs were then resuspended in toluene. The stable nano-colloid system of Au/toluene was then prepared for characterization. To confirm the size distribution and formation of the AuNPs, TEM techniques and UV-Vis absorption were used. The absorption maximum was found to be 524 nm, which is a shift typical for spherical AuNPs. This surface plasmon band agrees to 3–4 nm particles. According to the Mie theory, the purification procedure removed the
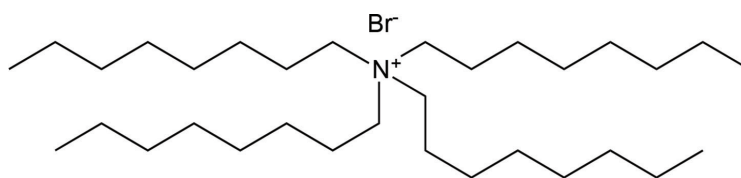

Figure 10.
TOAB chemical structure.

low-molar-mass impurities without essentially varying the structure of the NPs. The AuNPs were basically spherical and monodispersed with diameters around 3–4 nm.

Authors discussed an easy method to prepare dodecanethiol-stabilized AuNPs through a new microemulsion TOAB cationic surfactant-based system. This approach was related with the liquid-liquid phase method. Both AuNPs arranged by different procedures were studied with UV-Vis spectroscopy and TEM imaging, denoting good steadiness. The TEM images of the thiol-capped AuNPs ready by the microemulsion method showed a more acute monodispersity related to that prepared using the Brust method. Since all the methods could be carried out in one step, the microemulsion procedure was faster and easier.

5. Conclusions

As this review chapter has stated, microemulsion method must be taken into account when the aim of the researcher is to prepare well-controlled, narrow-sized, monodispersed NPs.

The influence of microemulsion components has been reviewed; not only the ratio between aqueous phase/surfactant and surfactant/metal precursor but also the influence of the nature of the surfactant—ionic, cationic, and nonionic surfactants—will offer different self-assembled systems. It was underlined that hydrodynamic radius (r_W = 1.5 W) of the microdroplets that forms the microemulsion essentially depends on W = [water/surfactant] so the size of our template will be defined by this relation and microdroplet will offer a well-defined microenvironment to prepare NPs. The influence of the tensioactive nature was also considered by the interaction with metal precursors, co-surfactant, during the nucleation and growth processes and consequent influence upon surficial charge of the NPs. Thus the influence of the reagents and its proportions or ratio will determine the size of water pool within the microdroplets, which finally determine size, shape, morphology, and crystalline structure of the NPs. The control of the reaction time, the temperature, and reagent nature and ratios between them will give us a production of different geometries that will find different applications in wide range of research fields, such as chemical sensors, CO sensing, applications on drug delivery and theranostic, quantum dots, MRI, and biomedicine. It can be concluded that microemulsion method actually offers a good route for synthesis of NPs.

Acknowledgements

Conflict of interest

Author does not declare conflict of interest.

Appendices and nomenclature

NPs	nanoparticles
MNPs	metal nanoparticles
QDs	quantum dots
MIONPs	magnetic iron oxide NPs
AOT	sodium bis(2-ethylhexyl)sulfosuccinate
SDS	sodium dodecyl sulfate
CTAB	cetyltrimethylammonium bromide
HTBA	hexadecyltrimethylammonium bromide
Triton X-100	4-(1,1,3,3-tetramethylbutyl)phenyl-polyethylene glycol
TOAB	tetraoctylammonium bromide
CMC	critical micelle concentration
DBS	sodium dodecylbenzene sulfonate
W/O	water-in-oil microemulsion
O/W	oil-in-water microemulsion
W	water/surfactant ratio
TEM	transmission electron microscopy
AGM	alternating gradient magnetometry
XRD	X-ray diffraction
DLS	dynamic sight scattering
EFTEM	energy filter transmission electron microscopy
XPS	X-ray photoelectron spectroscopy
UV-vis	UV-vis spectroscopy

Author details

Antonio Cid[1,2]*

1 Physical Chemistry Department, Faculty of Sciences, University of Vigo, Ourense, Galicia, Spain

2 UCIBIO@REQUIMTE, Chemistry Department, Faculdade de Ciências e Tecnologia, Universidade Nova de Lisboa, Caparica, Portugal

*Address all correspondence to: acids@fct.unl.pt

IntechOpen

References

[1] Lu A, Salabas EL, Schüth F. Magnetic nanoparticles: Synthesis, protection, functionalization, and application. Angewandte Chemie, International Edition. 2007;**46**:1222-1244. DOI: 10.1002/anie.200602866

[2] Bandow S, Kimura K, Kon-No K, Kthara A. Magnetic properties of magnetite ultrafine particles prepared by *W/O* microemulsion method. Japanese Journal of Applied Physics. 1987;**26**(5):713-717

[3] López-Quintela MA, Rivas J. Chemical reactions in microemulsions: A powerfull method to obtain ultrafine particles. Journal of Colloid and Interface Science. 1993;**158**:446-451

[4] Astray G, Cid A, García-Río L, Hervella P, Mejuto JC, Pérez-Lorenzo M. Organic reactivity in AOT-stabilized microemulsions. Progress in Reaction Kinetics and Mechanism. 2008;**33**:81-97. DOI: 10.3184/146867807X273173. ISSN: (1468-6783)

[5] Cid-Samamed A, García-Río L, Fernández D, Mejuto JC, Morales J, Pérez M. Influence of n-alkyl acids on the percolative phenomena in AOT-based microemulsions. Journal of Colloid and Interface Science. 2008;**318**(2):525-529. DOI: 10.1016/j. jcis.2007.11.001. ISSN: (0021-9797)

[6] Serxio IA, Cid A, García-Río L, Mejuto JC, Morales J. Influence of polyethylene glycols on percolative phenomena in AOT microemulsions. Colloid & Polymer Science. 2010;**288**(2):217-221. DOI: 10.1007/s00396-009-2122-0. ISSN: (0303-402X)

[7] Cid A, Astray G, Manso JA, Mejuto JC, Moldes OA. Artificial Intelligence for electrical percolation of AOT-based microemulsions prediction. Tenside, Surfactants,

Detergents. 2011;**48**(6):477-483. DOI: 10.3139/113.110155. ISSN: (0932-3414)

[8] Cid A, Gómez-Díaz D, Mejuto JC, Navaza JM. Viscosity and percolative phenomena in AOT based microemulsions. Tenside, Surfactants, Detergents. 2011;**48**(2):165-168. DOI: 10.3139/113.110119. ISSN: (0932-3414)

[9] Montoya IA, Astray G, Cid A, Manso JA, Moldes OA, Mejuto JC. Influence prediction of small organic molecules (ureas and thioureas) upon electrical percolation of AOT-based microemulsions using artificial neural networks. Tenside, Surfactants, Detergents. 2012;**49**(4):316-320. DOI: 10.3139/113.110197. (ISSN: 0932-3414)

[10] Li M, Schnablegger H, Mann S. Coupled synthesis and self-assembly of nanoparticles to give structures with controlled organization. Nature. 1999;**402**:393-395. DOI: 10.1038/46509

[11] Hopwood JD, Mann S. Synthesis of barium sulfate nanoparticles and nanofilaments in reverse micelles and microemulsions. Chemistry of Materials. 1997;**9**:1819-1828

[12] Liu ZL, Wang X, Yao KL, Du GH, Lu QH, Ding ZH, et al. Synthesis of magnetite nanoparticles in *W/O* microemulsion. Journal of Materials Science. 2004;**39**:2633-2636

[13] He H-w, Liu T, Chen YX, Cheng DJ, Li XR, Xiao Y, et al. Calcium carbonate nanoparticle delivering vascular endothelial growth factor-C siRNA effectively inhibits lymphangiogenesis and growth of gastric cancer in vivo. Cancer Gene Therapy. 2008;**15**:193-202. DOI: 10.1038/sj.cgt.7701122

[14] Cid A, Mejuto JC, Orellana PG, López O, Rial R, Simal-Gandara J. Effects of ascorbic acid on the microstructure and properties of

SDS micellar aggregates for potential food applications. Food Research International. 2013;**50**(1):143-148. DOI: 10.1016/j.foodres.2012.10.009

[15] Cid A, Morales J, Mejuto JC, Briz-Cid N, Rial-Otero R, Simal-Gándara J. Thermodynamics of sodium dodecyl sulphate-salicylic acid based micellar systems and their potential use in fruits postharvest. Food Chemistry. 2014;**151**:358-363. DOI: 10.1016/j.foodchem.2013.11.076. (ISSN: 0308-8146, e-ISSN: 1873-7072)

[16] Chin AB, Yaacob II. Synthesis and characterization of magnetic iron oxide nanoparticles via *w/o* microemulsion and Massart's procedure. Journal of Materials Processing Technology. 2007;**191**:235-237

[17] Chin AB, Yaacob II. Synthesis and characterization of iron oxides nanoparticles. Key Engineering Materials. 2006;**306-608**:1115-1120

[18] Bee A, Massart R, Neveu S. Synthesis of very fine maghemite particles. Journal of Magnetism and Magnetic Materials. 1995;**149**:6-9

[19] Shen M, Du Y, Yang P, Jiang L. Morphology control of the fabricated hydrophobic gold nanostructures in *w/o* microemulsion under microwave irradiation. Journal of Physics and Chemistry of Solids. 2005;**66**:1628-1634. DOI: 10.1016/j.jpcs.2005.05.078

[20] Sharma S, Pal N, Chowdhurry PK, Sen S, Ganguli AK. Understanding growth kinetics of nanorods in microemulsion: A combined fluorescence correlation spectroscopy, dynamic light scattering, and electron microscopy study. Journal of the American Chemical Society. 2012;**134**:19677-19684. DOI: 10.1021/ja306556e

[21] Sanchez-Dominguez M, Boutonnet M, Solans C. A novel approach to metal and metal oxide nanoparticle synthesis: The oil-in-water microemulsion reaction method. Journal of Nanoparticle Research. 2009;**11**:1823-1829. DOI: 10.1007/s11051-009-9660-8

[22] Capek I. Preparation of metal nanoparticles in water-in-oil (*w/o*) microemulsions. Advances in Colloid and Interface Science. 2004;**110**:49-74. DOI: 10.1016/j.cis.2004.02.003

[23] Santra S, Tapec R, Theodoropoulou N, Dobson J, Hebard A, Tan W. Synthesis and characterization of silica-coated iron oxide nanoparticles in microemulsion: The effect of nonionic surfactants. Langmuir. 2001;**17**: 2900-2906. DOI: 10.1021/la0008636

[24] khiev PS, Huang NM, Radiman S, Ahmad Md S. Synthesis of NiS nanoparticles using a sugar-ester nonionic water-in-oil microemulsion. Materials Letters. 2004;**58**:762-767. DOI: 10.1016/j.matlet.2003.07.006

[25] Pineda-Reyes AM, Olvera ML. Synthesis of ZnO nanoparticles from water-in-oil (*w/o*) microemulsions. Materials Chemistry and Physics. 2018;**203**:141-147. DOI: 10.1016/j.matchemphys.2017.09.054

[26] Yamauchi H, Ishikawa T, Kondo S. Surface characterization of ultramicro spherical particles of silica prepared by *W/O* microemulsion method. Colloids and Surfaces. 1989;**37**:71-80. DOI: 0166-6622/89

[27] Lee S, Carr CS, Shantz DF. Anionic microemulsion-mediated low temperature synthesis of anisotropic silicalite-1 nanocrystals. Langmuir. 2005;**21**:12031-12036. DOI: 10.1021/la052181u

[28] Astray G, Cid A, Manso JA, Mejuto JC, Moldes OA, Morales J. Basic degradation of 3-keto-carbofuran in the presence of non-ionic self-assembly colloids. Fresenius Environmental Bulletin. 2011;**20**(2):354-357

[29] Chen R, Han B, Yang L, Yang Y, Xu Y, Mai Y. Controllable synthesis and characterization of CdS quantum dots by a microemulsion-mediated hydrothermal method. Journal of Luminescence. 2016;**172**:197-200. DOI: 10.1016/j.jlumin.2015.12.006

[30] Wei Z, Lin X, Wu M, Zhao B, Lin R, Zhang Y, et al. Core-shell NaGdF$_4$@ CaCO$_3$ nanoparticles for enhanced magnetic resonance/ultrasonic dual-modal imaging via tumor acidic micro-enviroment triggering. Scientific Reports. 2017;**7**:5370. DOI: 10.1038/s41598-017-05395-w

[31] Zhou C, Chen T, Wu C, Zhu G, Qiu L, Cui C, et al. Aptamer-CaCO$_3$ nanostructures: A facile, pH-responsive, specific platform for targeted anticancer theranostics. Chemistry, an Asian Journal. 2015;**10**(1):166-171. DOI: 10.1002/asia.201403115

[32] Majumder D, Roy S. Development of low-ppm CO sensors using pristine CeO$_2$ nanospheres with high surface area. ACS Omega. 2018;**3**:4433-4440. DOI: 10.1021/acsomega.8b00146

[33] Wang H, Agarwal P, Zhao S, Yu J, Lu X, He X. A biomimetic hybrid nanoplatform for encapsulation and precisely controlled delivery of theranostic agents. Nature Communications. 2016;**6**:10081. DOI: 10.1038/ncomms10081

[34] Cid Samamed A, Moldes ÓA, Diniz MS, Rodríguez-González B, Mejuto JC. Redispersion and self-assembly of C 60 fullerene in water and toluene. ACS Omega. 2017;**2**:2368-2373. DOI: 10.1021/acsomega.7b00049. ISSN 2470-1343

[35] Tianimoghadam S, Salabat A. A microemulsion method for preparation of thiol-functionalized gold nanoparticles. Particuology. 2018;**37**:33-36. DOI: 10.1016/j.partic.2017.05.007